Temperature–Concentration Behavior of Solutions of Polydisperse, Atactic Poly(methyl methacrylate) and Its Influence on the Formation of Amorphous, Microporous Membranes

P. Vandeweerdt and H. Berghmans*

Laboratory for Polymer Research, K. U. Leuven, Celestijnenlaan, 200 F, B-3001 Leuven, Belgium

Y. Tervoort

Department of Polymer Technology, Eindhoven University of Technology, P.O. Box 513, 5600 MB Eindhoven, The Netherlands

Received July 16, 1990; Revised Manuscript Received January 7, 1991

ABSTRACT: The temperature–concentration behavior of solutions of atactic poly(methyl methacrylate) in 1-butanol and cyclohexanol was investigated. A liquid–liquid demixing interferes with a glass transition. In the high-concentration region, outside the demixing region, T_g decreases with decreasing polymer concentration. For concentrations in the demixing region, a slight increase of T_g with decreasing polymer concentration is observed. This is ascribed to the influence of the polymer polydispersity on the concentration of the coexisting phases. The extent of this increase depends strongly on the polydispersity of the polymer and on the nature of the solvent. The combination of these two thermal transitions leads to the formation of amorphous, glassy gels at room temperature. After elimination of the solvent, different morphologies can be obtained. They range from glassy particle dispersions to porous, glassy materials. The morphology can be controlled by overall polymer concentration and cooling rate.

Introduction

Liquid–Liquid phase separation in polymer solutions has been used for many years in the preparation of crystalline microporous materials.[1-6] Later on it has also been applied to the preparation of amorphous materials such as atactic poly(methyl methacrylate) (a-PMMA) and atactic polystyrene.[2,7-10] Recently, the solution behavior responsible for this process has been analyzed in detail for the atactic polystyrene–decalin[11-13] system. The solidification of the solution on cooling is caused by the combination of a liquid–liquid (L–L) demixing and a glass transition (T_g). The product is a brittle material, composed of a porous, glassy phase in which the dilute phase is dispersed. Because these structures do not flow and are moderately resistant to deformation, they are called amorphous gels. Of course, they do not show the same elastic characteristics as do biopolymer gels obtained from, e.g., gelatin solutions.

This interference of a L–L demixing and a glass transition has already been suggested as a plausible mechanism for the gelation of solutions of noncrystallizable polymers.[14-16]

This gelation mechanism is rather simple. When a solution is cooled, the liquid–liquid demixing causes the formation of two solutions of different concentration in equilibrium. Because of the importance of the kinetic aspects of the demixing, a finely dispersed, multiphase system of the two solutions is obtained. At a certain temperature, the demixing curve intersects the glass transition–concentration (T_g–ϕ_2) curve and the concentrated phases vitrify. An amorphous gel is obtained if material continuity is realized throughout the solution by these glassy phases. This process can lead to the preparation of a variety of microporous structures.[17] The morphology and the size of the phases depend strongly on the overall starting concentration and the cooling procedure. The structures obtained by binodal and spinodal demixing show important differences.[13]

We describe here a detailed study of the behavior of a-PMMA in 1-butanol and cyclohexanol. Both systems show a demixing curve with an upper critical solution temperature. The study should provide a better insight into the mechanism of the thermoreversible gelation of these solutions and the formation of different morphologies.

Experimental Section

1. Materials. (a) Polymers. The characteristics of the different a-PMMA samples, prepared by radical polymerization, are reported in Tables I and II. In order to control its molecular weight, a-PMMA1 was synthesized in solution with triethylamine as the transfer reagent. a-PMMA2 was synthesized by bulk polymerization. The resulting polymer was ultrasonically degraded in order to reduce both its average molecular weight and its molecular weight distribution. a-PMMA3 was also prepared by bulk polymerization.

The three polymers differ in their average molecular weight and/or their distribution. These data, obtained from GPC measurements, are reported in Table I. These samples have almost the same tacticity (Table II).

(b) Solvents. The solvents used throughout this study were 1-butanol (UCB) and cyclohexanol (Aldrich).

2. Preparation of the Solutions. Concentrations are given in weight fractions (ϕ_2). Solutions for optical and morphological observations of about 1 mL were prepared in glass tubes with a diameter of 1 cm. Concentrations up to $\phi_2 = 0.15$ were used. Samples for calorimetric observations over the complete concentration range were prepared in large-volume DSC sample pans. A sample of 30–50 mg was used for each experiment.

3. Calorimetric Observations. Calorimetric observations were performed with a Perkin-Elmer DSC 2C, equipped with a thermal analysis data station at a scan rate of 5 °C/min.

4. Optical Observations. The solutions were cooled at about 0.5 °C/min, and the onset of opalescence, characteristic for the onset of L–L demixing, was observed by the naked eye. The temperature where the onset is observed will be reported in this paper as T_d.

5. Morphology. Morphological observations were made by a Cambridge Stereoscan 200 scanning electron microscope. Samples were homogenized at 90 °C and cooled to room temperature at about 5 °C/min unless stated otherwise. Then the

0024-9297/91/2224-3547$02.50/0

Table I
Molecular Weight and Molecular Weight Distribution for the Different a-PMMA Samples

sample	$M_w \times 10^{-5}$	$M_z \times 10^{-5}$	M_z/M_w
a-PMMA1	1.32	2.36	1.8
a-PMMA2	1.32	1.86	1.4
a-PMMA3	3.87	9.90	2.6

solvent was exchanged against isopropyl alcohol, which was then evaporated. This treatment should not affect the morphology in an appreciable way as the concentrated domains are in the glassy state.

Experimental Observations and Discussion

I. Thermoreversible Gels from Solutions of a-PMMA. During cooling of concentrated solutions of the different a-PMMA samples in both solvents, solidification of the solution occurs before room temperature is reached and it is accompanied by a whitening of the solution. The phenomenon is analogous to that observed with solutions of atactic polystyrene in decalin.[11] In order to identify the mechanism of this transition, a detailed study of the temperature–concentration (T–ϕ_2) behavior and its relation to the morphology of the gels was undertaken.

II. Calorimetric Study of the Temperature–Concentration Behavior. 1. a-PMMA1 in 1-Butanol. It has been shown that liquid–liquid demixing can easily be observed by differential scanning calorimetry.[11] This technique has been applied to the different a-PMMA samples. Two different concentration regions have to be considered.

A typical cooling and heating scan of a solution of a-PMMA1 in 1-butanol with $\phi_2 < 0.85$ is given in Figure 1. A broad exothermic signal is observed on cooling (Figure 1A) due to the demixing of the system into two liquid solutions. For high concentrations the two solutions will be dispersed and a multiphase system is obtained. The onset temperature (T_d) of this exotherm is 63 °C. The exotherm is followed by a change in specific heat caused by the glass transition of the polymer-rich phases.

On heating, two different phenomena are observed (Figure 1B). At 41 °C an increase of Cp, representing the onset of the glass transition, sets in. It is followed by a broad endothermic signal, which represents the remixing of the different liquid phases and extends to 70 °C.

When the same experiments are carried out with solutions of $\phi_2 > 0.85$, only a glass transition is observed.

The values of T_g and T_d are plotted as a function of ϕ_2 in Figure 2, which shows an interference of the liquid–liquid demixing with the T_g–ϕ_2 curve. It can be subdivided into two regions.

In region 1 ($0 < \phi_2 > 0.85$), T_d as a function of the concentration represents the flocculation curve of the polymer–solvent system. In this demixing region T_g decreases with increasing polymer content from 46 °C ($\phi_2 = 0.1$) to 39 °C ($\phi_2 = 0.85$). On the contrary, T_g increases with increasing polymer content in region 2 ($0.85 < \phi_2 > 1$).

The intersection point of the demixing curve and the glass transition–concentration curve is situated at $\phi_2 = 0.85$ and $T = 39$ °C.

The shape of the glass transition curve in region 2 can easily be understood in the frame of the general principles of polymer physical chemistry. Addition of a low molecular weight substance to a polymer decreases its T_g (region 2). The T_g–ϕ_2 curve can be calculated theoretically with a very good agreement between theory and experiment.[19]

The increase of T_g with decreasing polymer concentration in region 1 is therefore less straightforward. It can be understood, however, when considering the mechanism of demixing of a polydisperse polymer.

The liquid–liquid demixing of a polymer solution results in the formation of two liquid solutions of different concentrations in equilibrium. In the case of a monodisperse polymer, the flocculation curve corresponds to the binodal and all the solutions with different initial concentrations follow the same binodal on cooling. The concentration of the different liquid phases obtained by demixing at a certain temperature is independent of the initial concentration. When the temperature at the intersection is reached, the concentrated phases vitrify. Because of the constancy of the concentration of the concentrated phases, this temperature is independent of the initial concentration. Therefore, the T_g of the solution is constant over the whole concentration range in the demixing region. This was observed with monodisperse atactic polystyrene, dissolved in *trans*-decalin.[13]

A different situation is encountered when a polydisperse sample is used. The concentration of the two liquid phases obtained by demixing depends on the initial concentration. The flocculation curve no longer represents the binodal, and each concentration has its own coexisting lines.

The concentration of the polymer-rich phases, obtained by demixing, is higher than that represented by the flocculation curve.[20] The concentration of the polymer-poor phases is also higher than expected from the flocculation curve.[20] The difference between the flocculation curve and the coexisting lines decreases with increasing overall concentration for the polymer-rich phases.[20] Calculations also have shown that this difference decreases with decreasing temperature and becomes negligible at lower temperatures.[20] The flocculation curve in the polymer-rich region therefore represents the binodal at these lower temperatures. The temperature and concentration at the intersection with the T_g–ϕ_2 curve are then also independent of the initial concentration. Solutions of a polydisperse polymer will show a constant T_g in region 1 as can be seen from the results with polydisperse atactic polystyrene dissolved in *trans*-decalin.[11,13]

When the difference between the flocculation curve and the coexisting lines is not negligible at lower temperatures, T_g will no longer be constant in region 1. A lower initial concentration will result in a more concentrated polymer-rich phase, and the intersection with the T_g–ϕ_2 curve will occur at higher temperature. Consequently, T_g will increase with decreasing polymer content. These intersection points can be localized by drawing a horizontal line from the T_g at different concentrations to the T_g–ϕ_2 curve. The concentration at this intersection point corresponds to that of the concentrated domains when vitrification sets in. This is shown for two different overall concentrations in Figure 2 (dotted lines).

From these observations it is clear that the difference between the flocculation curve and the coexisting lines for solutions of a-PMMA in 1-butanol is not neglibible at lower temperature.

This point of view is supported by observations with a sample of narrow molecular weight distribution like a-PMMA2, which gives a similar phase diagram (Figure 3). The difference in molecular weight distribution does not influence the glass transition–concentration curve in region 2 ($\phi_2 > 0.85$), but a different behavior is observed in region 1. The decrease of T_g with increasing concentration is less pronounced for a-PMMA2. A decrease of

Table II
Tacticity[a] of a-PMMA Samples[18]

	^{1}H NMR			^{13}C NMR		
	a-PMMA1	a-PMMA2	a-PMMA3	a-PMMA1	a-PMMA2	a-PMMA3
iso	0.05	0.05	0.06	0.05	0.06	0.05
hetero	0.39	0.37	0.37	0.36	0.40	0.39
syndio	0.56	0.58	0.57	0.59	0.54	0.56

[a] Fraction of triads.

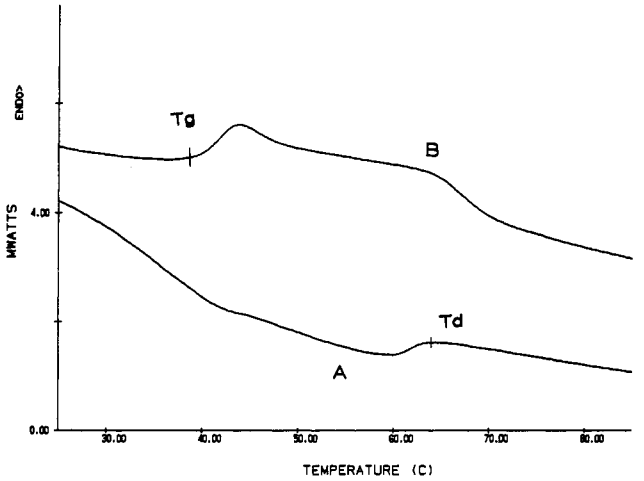

Figure 1. DSC cooling (A) and heating (B) scan of a solution of a-PMMA1 in 1-butanol (ϕ_2 = 0.59).

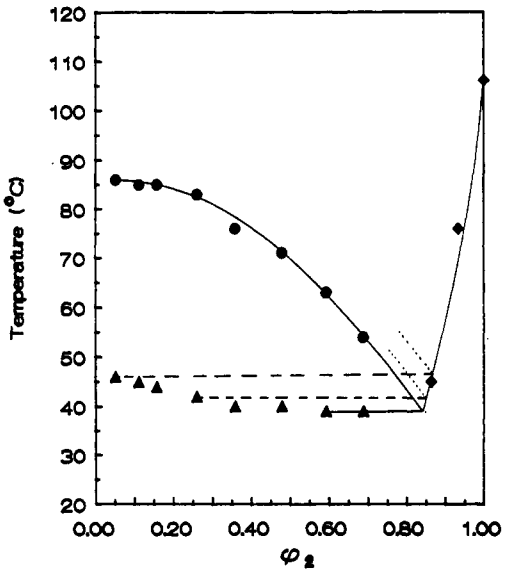

Figure 2. Temperature–concentration diagram for the system a-PMMA1/1-butanol: (▲) T_g, region 1; (♦) T_g, region 2; (●) T_d. (···) Coexisting lines derived from the T_g–ϕ_2 relation at ϕ_2 < 0.85, intersecting with the T_g–ϕ_2 line at ϕ_2 > 0.85.

only 3 °C is observed between ϕ_2 = 0.10 and ϕ_2 = 0.85. For a-PMMA1, this difference amounts to 7 °C. These data clearly reflect the influence of molecular weight distribution on the position of the coexisting lines.

The difference in distribution also influences the position of the flocculation curve. In the low-concentration range, demixing of a-PMMA1 sets in at higher temperatures than those observed with a-PMMA2. At higher concentrations (ϕ_2 > 0.3) the flocculation curves of a-PMMA1 and a-PMMA2 are identical.

Increasing the average molecular weight (a-PMMA3) does not affect the position of the maximum of the demixing curve (Figure 4). For higher concentrations demixing occurs at higher temperatures.

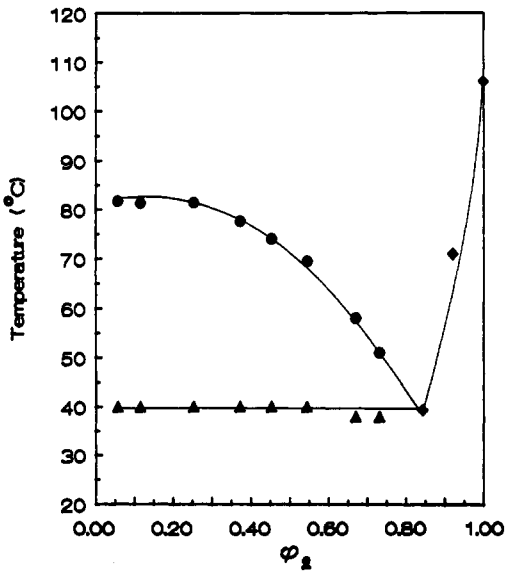

Figure 3. Temperature–concentration diagram for the system a-PMMA2/1-butanol: (▲) T_g, region 1; (♦) T_g, region 2; (●) T_d.

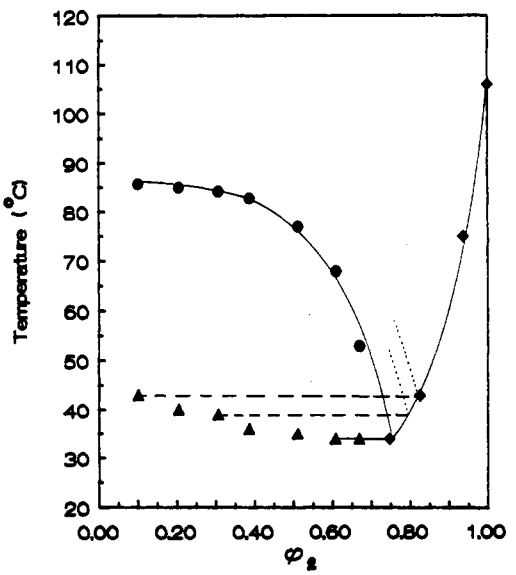

Figure 4. Temperature–concentration diagram for the system a-PMMA3/1-butanol: (▲) T_g, region 1; (♦) T_g, region 2; (●) T_d. (···) Coexisting lines derived from the T_g–ϕ_2 relation at ϕ_2 < 0.75, intersecting with the T_g–ϕ_2 line at ϕ_2 > 0.8.

The intersection of the flocculation curve with the glass transition curve occurs at about 34 °C and ϕ_2 = 0.75. This is 5 °C lower than that for a-PMMA1 and suggests a lower concentration in the polymer-rich phases. An important increase of T_g with decreasing ϕ_2 also occurs in the demixing region.

Consequently, the behavior of this polymer is very similar to that of a-PMMA1. The same conclusion can be drawn concerning the intersection of the coexisting curves and the T_g–ϕ_2 curve. These intersection points are also represented in Figure 4 for two different overall concentrations.

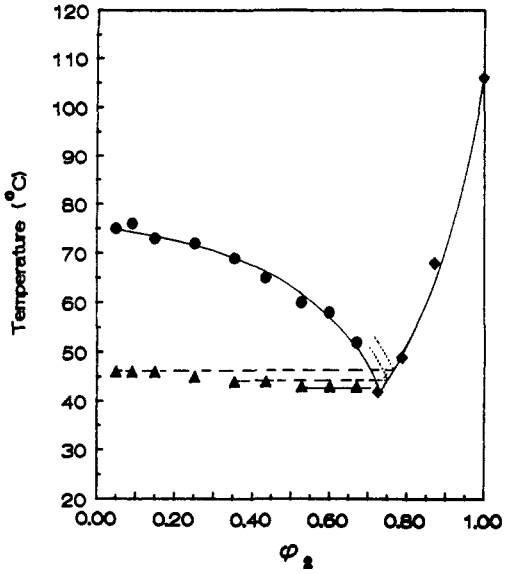

Figure 5. Temperature–concentration diagram for the system a-PMMA1/cyclohexanol: (▲) T_g, region 1; (♦) T_g, region 2; (●) T_d. (···) Coexisting lines as derived from the T_g–ϕ_2 relation at $\phi_2 < 0.75$, interesecting with the T_g–ϕ_2 line at $\phi_2 > 0.8$.

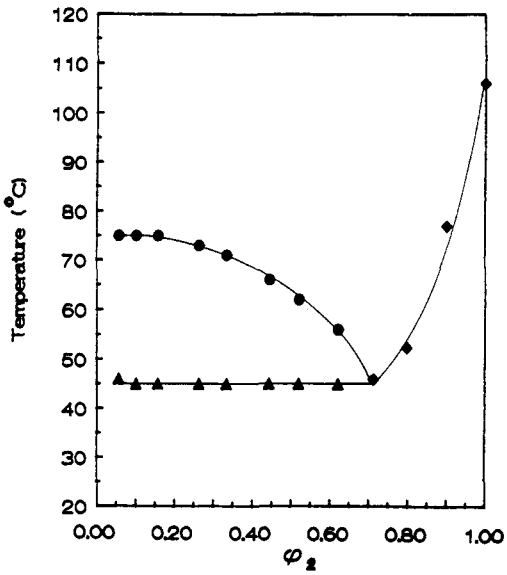

Figure 6. Temperature–concentration diagram for the system a-PMMA2/cyclohexanol: (▲) T_g, region 1; (♦) T_g, region 2; (●) T_d.

2. a-PMMA1 and a-PMMA2 in Cyclohexanol. The generality of the phenomena, reported in the previous paragraph, was further confirmed by observations made in cyclohexanol. The samples were studied in the same way, and the corresponding T–ϕ_2 diagrams are represented in Figure 5 (a-PMMA1) and Figure 6 (a-PMMA2). A great similarity exists with the data obtained in 1-butanol. Some differences have to be stressed.

The liquid–liquid demixing occurs at lower temperature for both samples. This is the direct consequence of the better solvent quality of cyclohexanol for a-PMMA.

In region 2, the decrease of T_g with decreasing concentration is less pronounced but is still independent of the molecular weight distribution.

The decrease of T_g with increasing polymer concentration in region 1 is strongly reduced for a-PMMA1 and almost absent for a-PMMA2. This means that the dependence of the concentration of the polymer-rich phases on the initial polymer concentration is smaller in cyclohexanol than in 1-butanol. The difference between the flocculation curve and the coexisting lines at lower temperature is therefore less pronounced than that for the system a-PMMA/1-butanol.

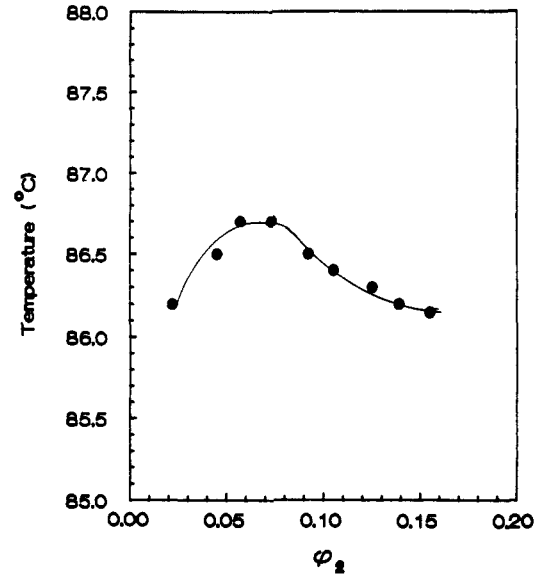

Figure 7. Flocculation curve of a-PMMA3 in 1-butanol obtained from optical observation (●, T_d).

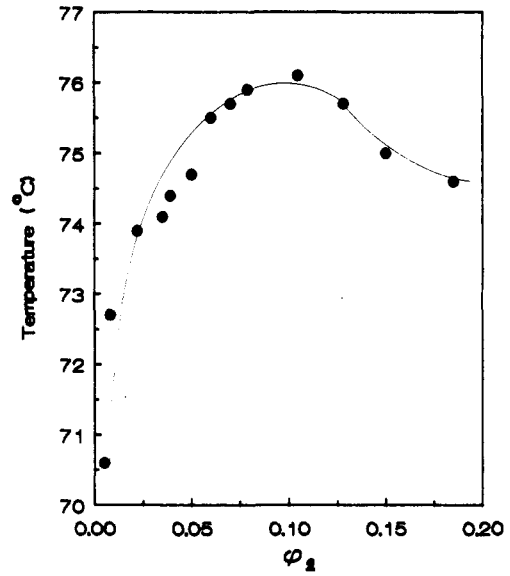

Figure 8. Flocculation curve of a-PMMA1 in cyclohexanol obtained from optical observations (●, T_d).

III. Optical Observations. In order to control the validity of the data observed by calorimetry, the optical behavior of solutions of some of these samples was investigated. For practical reasons they were performed with solutions of rather low concentration of a-PMMA3 in 1-butanol and of a-PMMA1 in cyclohexanol. The corresponding data are represented by the Figures 7 and 8.

A typical flocculation curve of a polydisperse polymer is obtained for a-PMMA3 in 1-butanol. It shows a maximum around $\phi_2 = 0.07$. The optical demixing curve is situated only 2° above the demixing curve obtained from DSC experiments. This can easily be understood by the different cooling rates used in the different experiments. The same conclusions can be drawn from a-PMMA1 in cyclohexanol, although the maximum is situated at $\phi_2 = 0.10$.

The excellent agreement between both observations confirms the validity of the DSC results for locating the

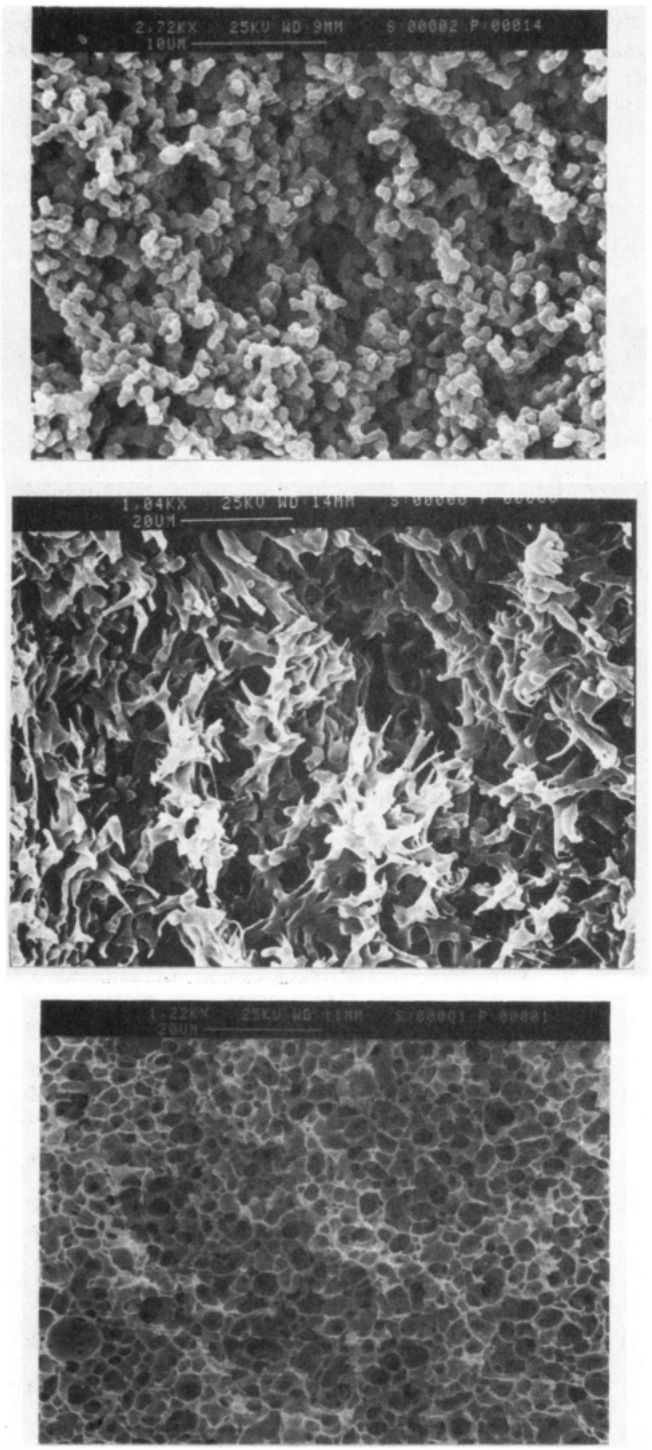

Figure 9. Scanning electron micrographs of demixed and vitrified solutions of a-PMMA1-butanol: (a) $\phi_2 = 0.05$, (b) $\phi_2 = 0.10$, (c) $\phi_2 = 0.15$.

demixing curve. But nevertheless DSC is not as accurate a measurement of the exact shape of the demixing curve or its maximum. This shortcoming can also be responsible for the difference between the optical and calorimetric results. Calorimetric observations constitute an easy method of detecting the occurrence of liquid–liquid demixing and of localizing its position on the temperature scale and are especially interesting at higher concentrations. Both methods are therefore complementary.

IV. Morphology. In order to produce the rigid, glassy, porous structures, mentioned previously, material continuity must be realized throughout the solution. The possibility of forming these structures and their relationship with the mechanism of demixing have been demonstrated recently.[13,14] The present work is a qualitative approach for illustrating the possibilities of the system a-PMMA/1-butanol. Consequently, no detailed discussion concerning the relationship between morphology and the mechanism of demixing will be given.

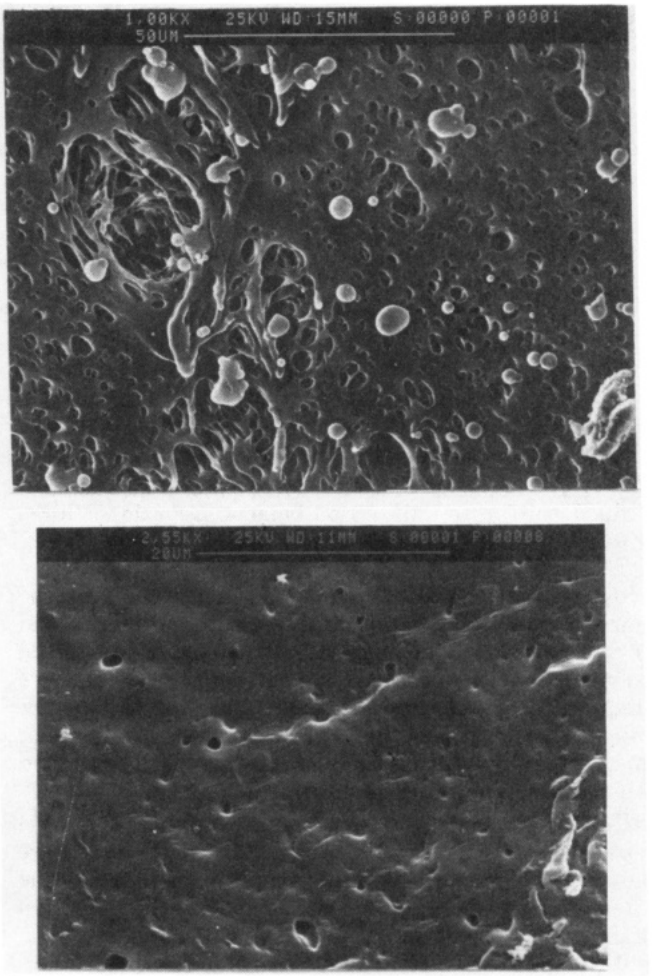

Figure 10. Scanning electron micrographs of demixed and vitrified solutions of a-PMMA1 in 1-butanol, cooled against a cold glass wall: (a) $\phi_2 = 0.10$, (b) $\phi_2 = 0.15$.

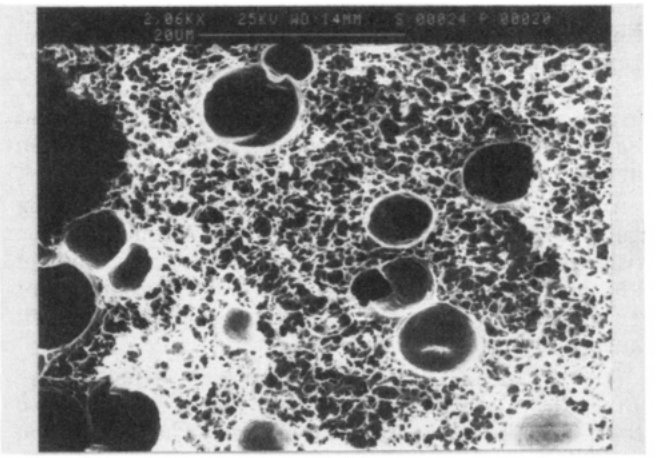

Figure 11. Scanning electron micrographs of a demixed and vitrified solution of a-PMMA3 in 1-butanol. Demixing was performed in two steps (see text).

The process is based on the vitrification of a demixed solution that evolves toward a macroscopic, two-phase system. Because of the specific nature of the demixing process (binodal or spinodal), a large number of concentrated and diluted phases are formed in the early stages of the demixing. This corresponds to a metastable

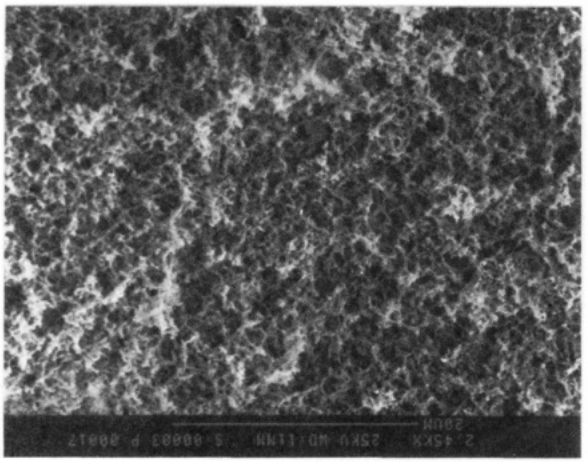

Figure 12. Scanning electron micrograph of a demixed and vitrified solution of a-PMMA3 in 1-butanol. Demixing occurred during quenching of the sample.

situation that can be frozen by vitrification before the macroscopic, two-layer situation is reached. The final degree of material continuity depends on the initial polymer concentration, which determines the relative amounts of concentrated and dilute phases. The structure will also be affected by the type of demixing: spinodal or binodal demixing. This problem, however, will be treated quantitatively in a future paper.

Cooling a solution of a-PMMA1 in 1-butanol ($\phi_2 = 0.05$) results in the formation of spherical glassy particles (Figure 9a). The rigidity of the solution mainly results from the interaction between the particles and causes the formation of pasty gels. Increasing the overall concentration to $\phi_2 = 0.1$ results in a bicontinuous morphology (Figure 9b), which suggests a spinodal mechanism. However, this could result from nucleation-controlled, binodal demixing that evolves into this bicontinuous structure. This will become even more pronounced at higher concentrations ($\phi_2 = 0.15$) (Figure 9c). From a detailed examination of this micrograph and others that will be discussed in a future paper, we can conclude that the bicontinuity is, at least partially, respected. It also became clear from these pictures that the morphology evolves toward a set of closed cells when the concentration is raised.

An asymmetric morphology can be obtained by cooling against a cold solid phase like a glass wall. From a solution with $\phi_2 = 0.1$, a porous morphology, covered by a compact skin, is obtained (Figure 10a). Although the skin is not yet continuous at $\phi_2 = 0.1$, it will be at higher overall concentration ($\phi_2 = 0.15$, Figure 10b).

With a-PMMA3 in 1-butanol, the same structures are obtained. A solution of $\phi_2 = 0.15$ was demixed in two steps. At higher temperatures, just below the flocculation curve, demixing seems to proceed by nucleation and growth (binodal demixing) and results in the formation of large spherical holes. On further cooling, bicontinuous porous structures probably originating from a spinodal process are formed (Figure 11).

Quenching of the samples in liquid nitrogen strongly reduces the pore size by an average factor of 8 (Figure 12). The overall shape of the morphology is not changed.

Conclusions

(1) The temperature–concentration behavior of a-PMMA in 1-butanol and cyclohexanol is characterized by the combination of a liquid–liquid demixing and a T_g–concentration curve.

(2) The intersection of these two curves indicates the formation of amorphous gels.

(3) The location of the intersection point of both curves depends on the molecular weight and on the polydispersity of the polymer.

(4) Porous membranelike morphologies can be obtained. The type of morphology and the average pore size depend on the initial concentration and the cooling conditions. The relationship with the binodal and/or spinodal demixing mechanism necessitates further investigations.

(5) Asymmetric membranes can be obtained by preparing these samples in contact with a glass wall.

Acknowledgment. We thank the IWONL for a fellowship for P.V. and the NFWO for financial support. We also thank Prof. P. Lemstra and H. Ladan of T.U. Eindhoven for their help with the morphological observations.

References and Notes

(1) Castro, A. J. U.S. Patent 4247498, Jan 27, 1981.
(2) Aubert, J. H.; Clough, R. L. *Polymer* **1985**, *26*, 2047.
(3) Aubert, J. H. *Macromolecules* **1988**, *21*, 3468.
(4) Young, A. T. *J. Vac. Sci. Technol.* **1986**, *4* (3), 1128.
(5) Young, A. T. *J. Cell. Plast.* **1987**, *23*, 55.
(6) Stoks, W.; Berghmans, H.; Moldenaers, P.; Mewis, J. *Br. Polym. J.* **1988**, *20*, 3468.
(7) Caneba, G. T.; Soong, D. S. *Macromolecules* **1985**, *18*, 2538.
(8) Caneba, G. T.; Soong, D. S. *Macromolecules* **1985**, *18*, 2545.
(9) Tsai, F. J.; Torkelson, J. M. *Polym. Mater. Sci. Eng.* **1989**, *61*, 789.
(10) Tsai, F. J.; Torkelson, J. M. *Macromolecules* **1990**, *23*, 3, 775.
(11) Arnauts, J.; Berghmans, H. *Polym. Commun.* **1987**, *28*, 66.
(12) Arnauts, J.; Berghmans, H. In *Polymer Networks*; Burchard, W., Ross-Murphy, Eds.; Elsevier Applied Science: 1990; Chapter 3, p 35.
(13) Arnauts, J.; Berghmans, H. To be published.
(14) Tan, H.; Moet, A.; Hiltner, A.; Baer, E. *Macromolecules* **1983**, *16*, 28.
(15) Wellinghof, S. T.; Shaw, J.; Baer, E. *Macromolecules* **1979**, *12*, 932.
(16) Boyer, R. F.; Baer, E.; Hiltner, A. *Macromolecules* **1985**, *18*, 427.
(17) Hikmet, R. M.; Callister, S.; Keller, A. *Polymer* **1988**, *29*, 1378.
(18) Bovey, F. A.; Tiers, G. V. D. *J. Polym. Sci.* **1960**, *44*, 173.
(19) Couchmann, P. R.; Karasz, F. E. *Macromolecules* **1987**, *11*, 117.
(20) Koningsveld, R. *Adv. Polym. Sci.* **1970**, *7*, 1.

Registry No. PMMA, 9011-14-7; 1-butanol, 71-36-3; cyclohexanol, 108-93-0.